Electrochimica Acta 205 (2016) 45–52

Contents lists available at ScienceDirect

Electrochimica Acta

journal homepage: www.elsevier.com/locate/electacta

A new probe into thin copper sulfide counter electrode with thickness below 100 nm for quantum dot-sensitized solar cells

Rui Xia[a], Shimao Wang[a], Weiwei Dong[a,b,*], Xiaodong Fang[a,b,c,**], Linhua Hu[b], Jun Zhu[b]

[a] Anhui Provincial Key Laboratory of Photonic Devices and Materials, Anhui Institute of Optics and Fine Mechanics, Chinese Academy of Sciences, Hefei 230031, China
[b] Key Lab of Novel Thin Film Solar Cells, Chinese Academy of Sciences, Hefei 230031, China
[c] School of Environmental Science and Optoelectronic Technology, University of Science and Technology of China, Hefei 230026, China

ARTICLE INFO

Article history:
Received 28 December 2015
Received in revised form 21 March 2016
Accepted 9 April 2016
Available online 12 April 2016

Keywords:
thickness
copper sulfide
counter electrode
chemical bath deposition
quantum dot-sensitized solar cell

ABSTRACT

Currently, most of CuS counter electrodes (CEs) used in quantum dot-sensitized solar cells (QDSSCs) are provided with a thickness of hundreds of nanometers or even several microns. Considering the CE with low thickness having many advantages, thin CuS films with thickness ranging from 47 nm below to 115 nm have been synthetized in this paper via chemical bath deposition (CBD) method with different bath concentrations. A power conversion efficiency (PCE) of 3.25% has been achieved utilizing CuS thin films a thickness of only 64 nm as CEs in QDSSCs without any structural optimization, which is higher than the value of the cell employing CuS CE with thickness of 2.8 μm. Electrochemical impedance spectroscopy, Tafel polarization, and two-point current-voltage measurements are used to investigate the electrocatalytic and conductive performance of CuS CEs with different thickness. Owing to the highest electrocatalytic capacity and good conductivity of the 64 nm-thick CuS CE, QDSSC assembled with this CE has reached relatively high PCE under one sun illumination (100 mW cm^{-2}, AM 1.5). In addition, cyclic voltammetry measurements indicate that the thin CuS CE has a good stability against the polysulfide electrolyte.

1. Introduction

Counter electrode (CE) is a vital part of quantum dot-sensitized solar cells (QDSSCs) [1,2]. For the efficient and compatible electrolyte containing S_n^{2-}/S^{2-} redox couples adopted in QDSSC, Pt CE widely used in dye-sensitized solar cells (DSSCs) has encountered bottlenecks in QDSSC applications due to the chemisorption of the sulfur atoms on its surface [3,4]. Therefore, various alternative materials such as Au [5], carbon [6,7], polymer [8], Cu_xS (x = 1 – 2) [9–13], PbS [14], CoS [15], Cu_2ZnSnS_4 [16], and some composite materials [17,18] have been reported as potential CEs. Among which, copper sulfide (Cu_xS, x = 1 – 2) materials appear to be a category of very suitable candidates with low cost, nontoxicity, and superior catalytic activity toward S_n^{2-}/S^{2-} redox couples [19,20]. Moreover, it is reported that CuS CEs tend to own higher conductivity, catalytic performance and be more stable compared with Cu_2S, $Cu_{1.8}S$, $Cu_{1.75}S$ and $Cu_{1.12}S$ CEs in QDSSCs [21,22].

Extensive researches about CuS CEs are mainly concentrated on creating novel structures or ameliorating preparation method. In general, the thicknesses of CuS films by different synthesis routes are mostly reported to be hundreds of nanometers or even several microns, and the corresponding power conversion efficiencies (PCE) of QDSSCs range from 2% to 5%. The group of Meng synthesized the CuS films on fluorine-doped tin oxide (FTO) glass using the chemical bath deposition (CBD) method combined with $TiCl_4$ treatment, the assembled QDSSCs obtained a PCE of 4.02% with 900 nm-thick CuS CEs [23]. Zhao et al. had compared the CuS CEs prepared through hydrothermal method with different thickness from 100 nm to 2 μm [24], Among them, QDSSC with 1 μm-thick CuS CE got the highest PCE of 3.65%, while the PCE of QDSSC using 100 nm-thick CuS CE was 1.75%. Little attention has been devoted to the CuS CE with thickness below or around 100 nm. Nevertheless, CE with small thickness have many advantages, such as saving materials usage, avoiding hindering the charge transfer from being too thick [25], and strong

* Corresponding authors at: Anhui Institute of Optics and Fine Mechanics, Chinese Academy of Sciences, Hefei 230031, China. Tel.: +86 551 65593508.
** Corresponding authors at: Anhui Institute of Optics and Fine Mechanics, Chinese Academy of Sciences, Hefei 230031, China.
Tel: +86 551 65593661; fax: +86 551 65593665.
E-mail addresses: wwdong@aiofm.ac.cn (W. Dong), xdfang@aiofm.ac.cn (X. Fang).

http://dx.doi.org/10.1016/j.electacta.2016.04.047
0013-4686/

attachment to the substrate and other materials. Previous research have revealed that Pt CEs with thickness of only 2 nm are sufficient to catalyze the electrolyte in DSSC [25]. Therefore, it is important to study whether CuS CEs with small thickness can also give a high catalytic performance towards the S_n^{2-}/S^{2-} electrolyte in QDSSCs.

In this paper, CBD method was used to grow CuS thin films due to its simplicity and good repeatability, different CuS thin films with thickness from 47 nm below to 115 nm were fabricated on FTO glass as CEs. The effects of bath concentration on the thickness, surface morphology, optics, and conductivity properties were studied in detail. The corresponding photovoltaic performance, electrochemical catalytic activity, and stability towards S_n^{2-}/S^{2-} redox couple of CuS CEs were investigated. Among them, QDSSCs assembled with 64 nm-thick CuS CEs acquired the highest PCE of 3.25%. To the best of our knowledge, it is the highest PCE of QDSSCs using such thin CuS CEs.

2. Experimental details

2.1. Preparation of copper sulfide thin films

The CuS thin films were prepared by CBD method on FTO (TEC-8, 8 Ω sq^{-1}, LOF) substrates. The FTO glasses were ultrasonically cleaned with distilled water, acetone, and ethanol then dried in N_2 atmosphere. The chemical bath used for synthesizing the CuS thin films was prepared as follows: an aqueous solution of 20 ml of 0.025 M of copper(II) sulfate pentahydrate ($CuSO_4{\cdot}5H_2O$) and a 20 ml of 0.05 M of sodium citrate ($C_6H_5Na_3O_7$) were mixed at first, the pH of the solution was adjusted to 1.5 with dilute sulfuric acid, then, 8 ml of 0.025 M of sodium thiosulfate pentahydrate ($Na_2S_2O_3{\cdot}5H_2O$) aqueous solution was added in the above solution, a clear solution was obtained. FTO substrates were dipped into the above solution, and heated to 75 °C for 60 min, the as-synthesized CuS film was labeled as CS 1. To investigate the effect of the precursor solution on synthesized films, CS 2, CS 2.5, CS 3, and CS 3.5 were prepared by multiplying the concentration of precursor solution components, respectively. The concentration parameters of bath solution are shown in Table 1. Relatively thick CuS films prepared by doctor blading (labeled as CS-DB) were used as reference, the slurry was prepared according to the previous report [26], specifically, two kinds of ethyl cellulose (EC) powders, i.e., EC (5–15 mPa s) and EC (30–60 mPa s) were dissolved in ethanol to obtain 10 wt% solutions, herein, they were labeled as M9 and M70, respectively. 0.5 g CuS powders scrapped from the as-prepared films were added into 2.5 g terpineol, 1.2 g M9, and 1.2 g M70, after stirring for 12 h, the prepared slurry was scraped on FTO substrate, then they were annealed at 370 °C in air for 30 min in tube furnace.

2.2. Preparation of CdS/CdSe co-sensitized TiO_2 films

TiO_2 nanoparticle films with optimized thickness of 10 μm fabricated via screen printing on FTO substrates were used as the photoanodes. The matrix of photoanode was prepared simply by the commercial TiO_2 nanoparticles (Degussa P25) without casting a scattering layer of large TiO_2 particles or any other TiO_2 structural optimization. The CdS and CdSe QDs were deposited onto TiO_2 photoanode in turn through successive ionic layer absorption and reaction (SILAR) processes according to our previous work [27,28]. In brief, 7 CdS cycles and 4 CdSe cycles were adopted to co-sensitize TiO_2 photoanode. After CdS/CdSe co-sensitization, the samples were coated with ZnS passivation layer via dipping alternately into 0.5 M $Zn(NO_3)_2$ ethanol solution and 0.2 M Na_2S methanol solution for 2 min each.

Table. 1
Concentration parameters of precursor solution, thickness, RMS parameters of CS 1, CS 2, CS 2.5, CS 3, and CS 3.5.

Sample name	$CuSO_4$ (M)	$Na_2S_2O_3$ (M)	Sodium citrate (M)	Thickness (nm)	RMS (nm)
CS 1	0.025	0.025	0.05	*	25.4
CS 2	0.05	0.05	0.1	47 ± 6	19.8
CS 2.5	0.0625	0.0625	0.125	64 ± 3	18.4
CS 3	0.075	0.075	0.15	92 ± 5	19.5
CS 3.5	0.0875	0.0875	0.175	115 ± 7	29.4

* thickness of CS 1 was too thin for step profiler to be measured.

2.3. QDSSCs assembly

The CdS/CdSe co-sensitized TiO_2 photoanode with an effective area of 0.25 cm^2 and different CEs (CS 1, CS 2, CS 2.5, CS 3, CS 3.5, CS-DB, and Pt) were separated by hot-melt Surlyn films then sealed through hot-pressing. Pt CEs were prepared via scraping H_2PtCl_6 solution onto FTO substrate and heated in air at 410 °C for 30 min [29]. The redox electrolyte consisting of 1 M Na_2S, 1 M S and 0.2 M KCl in water/methanol (3:7 by volume) was injected into the interspace between the photoanode and the CEs from the CEs side through a predrilled hole.

2.4. Measurements

The crystal structure of prepared films was examined by X-ray diffraction (XRD) using an X-ray diffractometer (Philips X'pert, Holland) with CuKa radiation (λ = 1.5418 Å). The surface morphology of the CuS films were characterized using a field-emission scanning electron microscope (FE-SEM; FEI Sirion-200, USA), the chemical composition of synthesized films were determined using the energy dispersive X-ray spectroscopy (EDX). Surface conditions and root mean square roughness of films were acquired using atomic force microscope (AFM, CSPM-5500, China), and the measured area is 16 μm × 16 μm. The thickness of the films was determined with a step profiler (XP-2, AMBIOS Technology Inc., USA). UV-visible absorption spectra were recorded by a double beam UV-visible spectrophotometer (U-3900H, Japan) in the wavelength range from 200 to 900 nm.

The photovoltaic performance of QDSSCs was measured with a Keithley 2420 digital source meter under irradiation of a solar simulator (Newport Oriel 94043A, USA, AM1.5, 100 mW cm^{-2}). The irradiation intensity was calibrated with standard crystalline silicon solar cell (Oriel, Newport, USA). For cell devices prepared under each condition, at least 4 cells were prepared and tested in parallel. The total active area of QDSSCs was 0.25 cm^2. The monochromatic incident photon-to-current conversion efficiency (IPCE) spectra were measured using 300 W Xe lamp light source with monochromatic light from 300 to 800 nm.

The current–voltage (*I–V*) measurements were conducted in dark, several gold electrodes with thickness of around 50 nm were evaporated on CuS films, and the measured sample area is 13 mm × 18 mm. Electrochemical impedance spectroscopy (EIS) was obtained by applying sinusoidal perturbations of ±5 mV over the bias 0.5 V at frequencies from 10^5 Hz to 0.1 Hz on the electrochemical workstation (CHI660A, CH Instruments, Inc. Austin, TX), using the symmetrical cells at room temperature in the dark. The composition of electrolyte used for EIS measurement was identical to that used in the cell devices. Tafel plots and cyclic voltammetry (CV) were also measured on the electrochemical work station using symmetrical cells, the scan rate of Tafel measurements was 10 mV s^{-1}, and the CV test was cycled 30 times from −0.65 V to 0.65 V with a scan rate of 0.1 V s^{-1}.

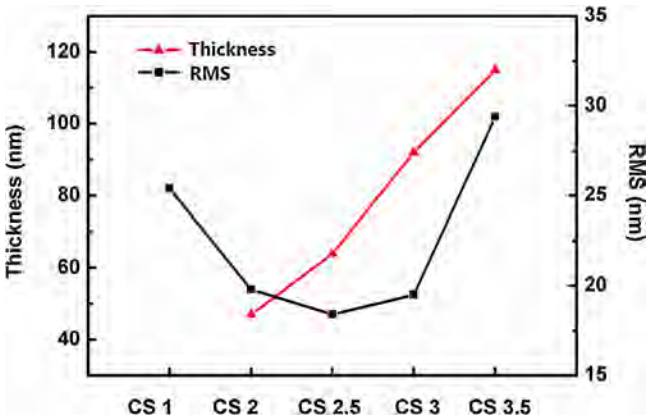

Fig. 1. The thickness and RMS of prepared films.

3. Results and discussion

3.1. Microstructure

The formation mechanism of the film has been described as the slow release of sulfur ions from $Na_2S_2O_3$ and then combines with copper complex ions in an acid solution [11], since the rough surface of FTO substrate is favorable for the nucleation of CuS, CuS films are deposited only on the side with FTO-coated layer. During the whole reaction process, pH value of the reaction solution is crucial for the growth of CuS thin film. In our experiments, the prepared films with pH value over 2.0 can be easily peeled off from the substrate, and they are hard to grow on the FTO substrate when the pH value is below 1.0. Therefore, the pH value of 1.5 is adopted.

Concentration of precursor solution is another important factor for films growth, different concentration of precursor solutions is used to change the thickness of the films. Thickness parameters of CuS films, acquired by step profiler, are listed in Table 1, and the thickness of CS 1 is too thin to obtain a valid data. From CS 2 to CS 3.5, the films become thicker with the increase of the

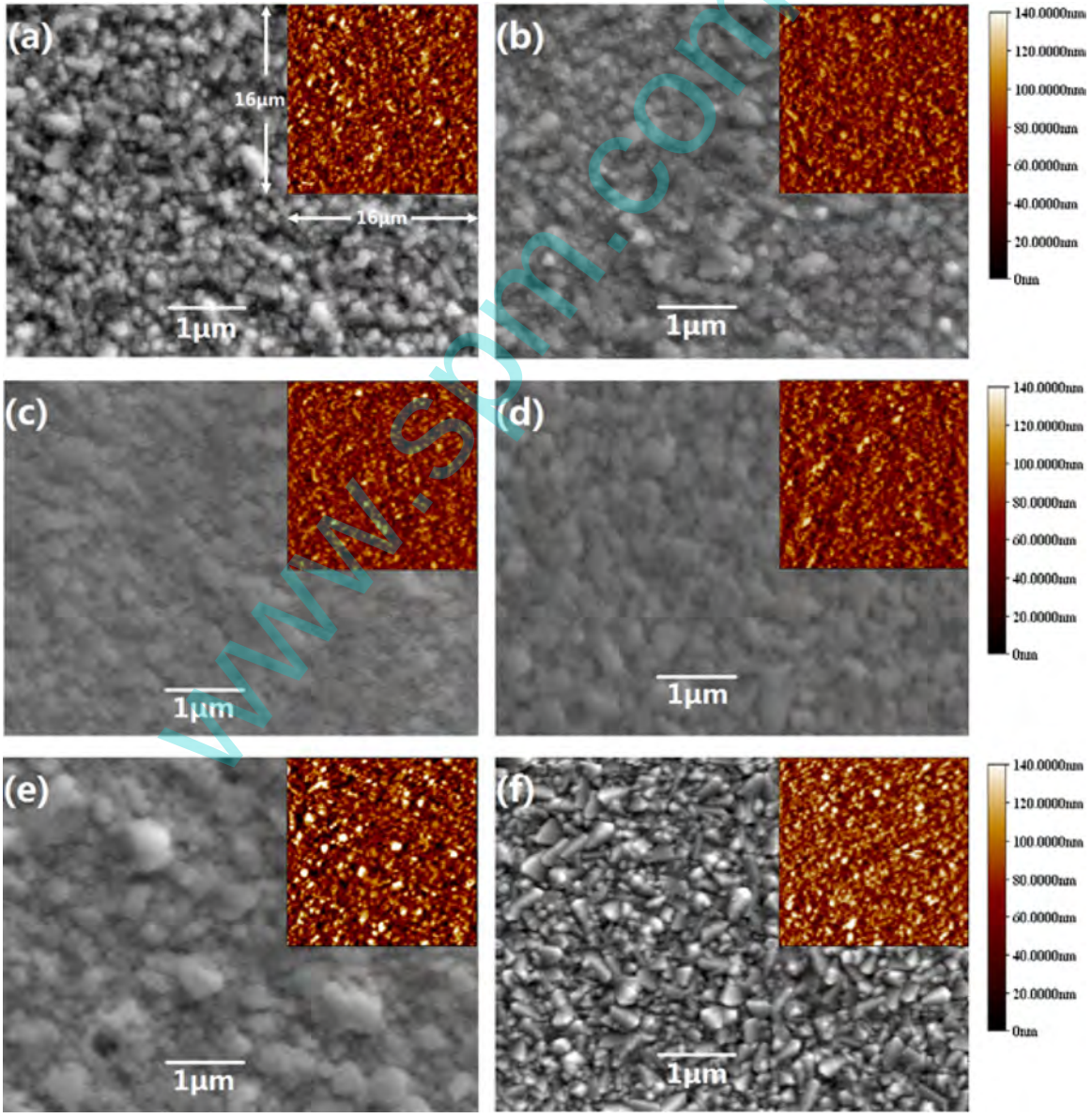

Fig. 2. SEM images of (a) CS 1, (b) CS 2, (c) CS 2.5, (d) CS 3, (e) CS 3.5, and (f) FTO. The inset is their corresponding AFM image.

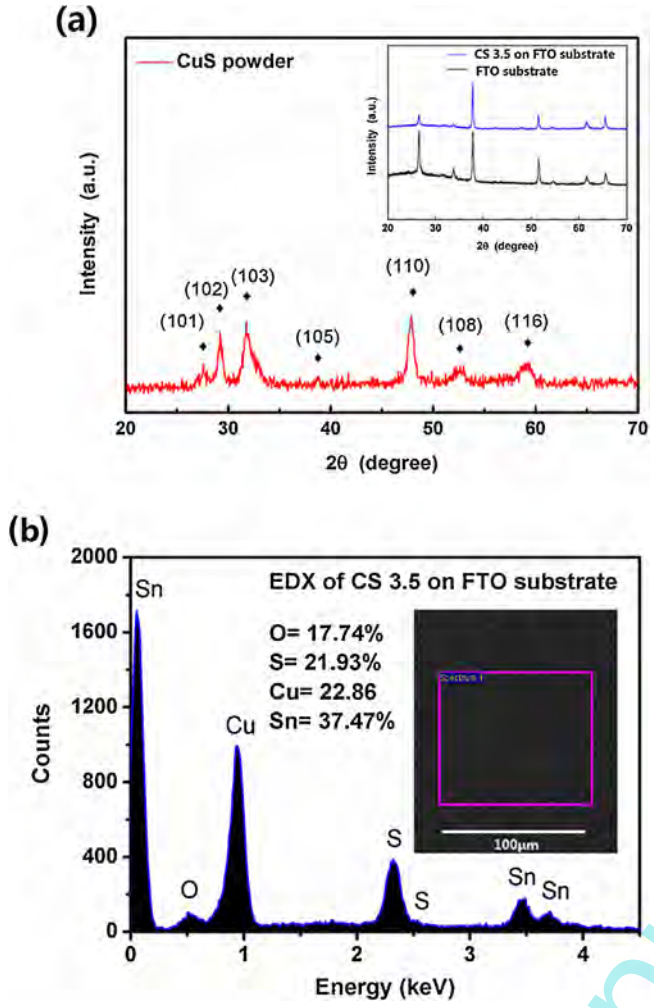

Fig. 3. (a) XRD patterns of scraped off CuS powders, the inset is the XRD pattern of the CS 3.5 on FTO and FTO substrate. (b) EDX spectrum of CS 3.5 on FTO substrate, the inset is the measured area of CuS films under EDX instrument.

concentration of precursor solution and the trend of thickness growth tends to be linear according to Fig. 1, the maximum thickness film of CS 3.5 is about 115 nm.

Fig. 2 demonstrates the SEM images of CuS thin films prepared with different precursor solution. They show the CuS thin films on the FTO substrate are actually made of many tiny articles, and the composed particles become smaller and more uniform from CS 1 to CS 2.5. From CS 2.5 to CS 3.5, the particles grow larger and less consistent. For comparison, AFM images of each sample are also exhibited and the corresponding root mean square (RMS) roughness parameters are shown in Table 1. The *RMS* value of CS 1 is 25.4 nm, which is similar to that of FTO substrate (26.1 nm), inferring that the films is too thin to fully cover the substrate. With increasing the bath concentration from CS 2 to CS 3.5, the variation trend of *RMS* value is depicted in Fig. 1, the RMS value of CS 2.5 is raised to minimum value (18.4 nm) while that of CS 3.5 is increased to maximum value (29.4 nm).The same tendency can be also observed from the AFM images in the insert of Fig. 2. Explicitly, there are lots of large particles on the surface of CS 3.5, which is consistent with the SEM images.

By combining the growth mechanism of CBD [30,31], the variation in RMS value of different films can be explained as follows: when the bath concentration is low, the CuS particles are prior to nucleate at the concave parts of FTO surface which have relatively low nucleation energy [32,33]. As the bath concentration increase, the formed CuS particles grow and merge together, blocking in the concave parts, the RMS value decreases. With further increasing the precursor solution, the FTO surface is completely covered by CuS films, the new grown CuS particles randomly appear on the formed CuS films, and the RMS value bounces to increase.

3.2. Structural characterization

Phase structure results identified by XRD measurements are exhibited in Fig. 3 (a). Since the CuS films obtained by CBD are used without further thermal annealing, the crystallization is poor, even the XRD diffraction peaks of the CS 3.5 with the highest thickness are hard to be observed according to the inset of Fig. 3 (a). Powders scraped off from the film are collected and measured. (101), (102), (103), (105), (110), (108), and (116) peaks are clearly visible and no other peaks are found in Fig. 3 (a), which corresponds to the pure hexagonal CuS phase (JCPDS: 6 – 464). The EDX spectrum of CS 3.5 in Fig. 3 (b) show the presence of Cu (22.86%) and S (21.93%) elements with atomic ratios close to the stoichiometry of CuS. The atomic ratios of other samples are also close to 1:1, indicating the formation of CuS films further.

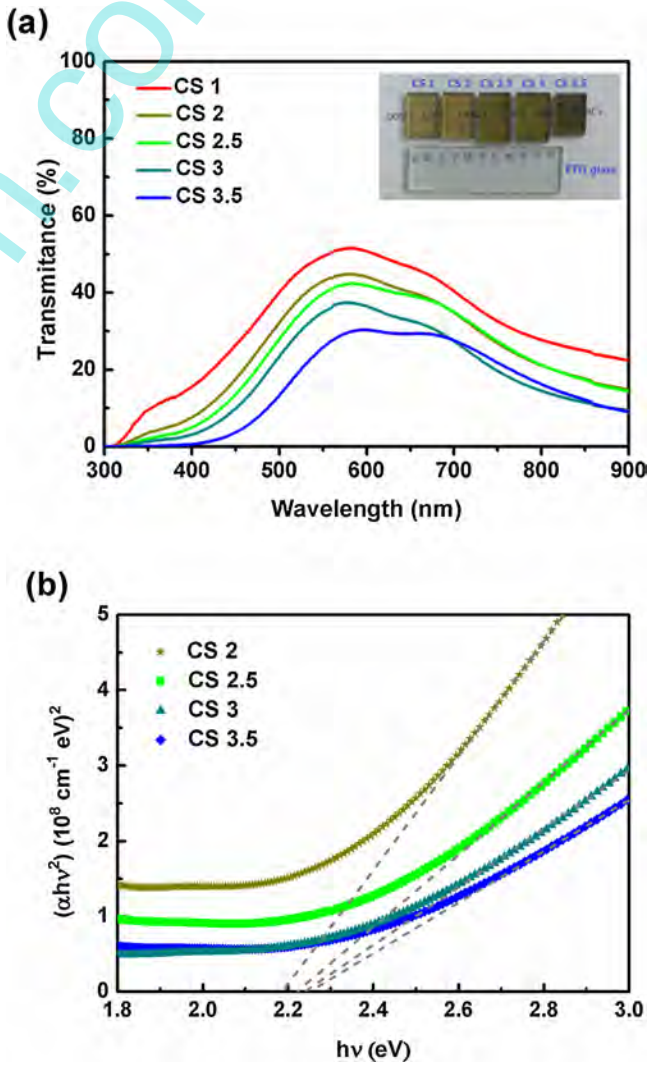

Fig. 4. (a) Transmittance spectra of CuS films with different bath concentration, the inset is the digital photographs of different CuS films; (b) $(\alpha h\nu)^2$ vs $h\nu$ plots of the CuS films.

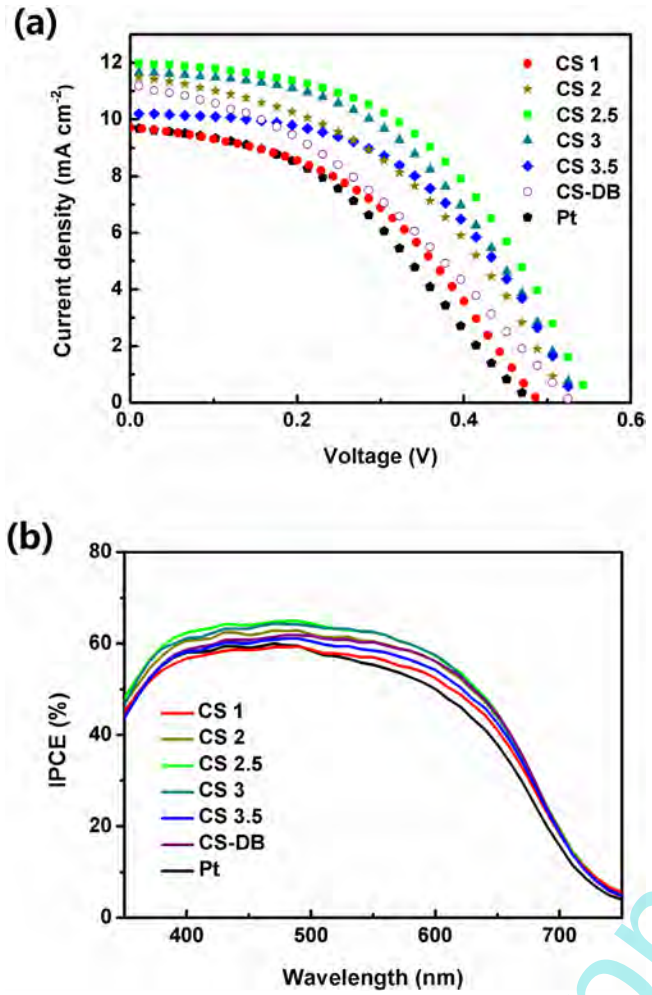

Fig. 5. (a) The *J-V* curves of QDSSCs employing different CEs. (b) IPCE spectra of QDSSCs based on different CEs.

3.3. Optical properties

The transmittance spectra of CuS films with different bath concentration are shown in Fig. 4 (a), and their digital photographs are exhibited in the inset. With the increase of bath concentration, the films become thicker and the color of the films tends to be darker, which results in the reduction of transmittance. The decrease in the transmittance at wavelength shorter than 800 nm is attributed to the intrinsic band gap absorption of CuS, the optical band gap derived from Tauc's relation [34]:

$$(ahv)^2 = A(hv - E_g)^2 \quad (1)$$

are shown in Fig. 4 (b). Where A is the optical transition dependent constant, E_g is the optical energy band gap. The deduced optical band gap values are all close to 2.20 eV, which is similar with the optical band gap value of CuS thin films reported in the literature [35,36].

3.4. Photovoltaic performance

Fig. 5 (a) demonstrates the photocurrent density – voltage ($J-V$) characteristics of the QDSSCs assembled with different CuS and Pt CEs, and the photovoltaic parameters derived from the $J-V$ curves are summarized in Table 2. On the overall point of view, the QDSSCs with CuS CEs perform better photoelectric properties than the cells with Pt CEs, which is due to the higher electrocatalytic capacity towards S_n^{2-}/S^{2-} redox couples of CuS CEs than that of Pt CEs. Among the solar cells using CuS CEs, most of the thin CuS CEs based QDSSCs are comparable and even better in the photovoltaic parameters compared with the thick CS-DB based QDSSCs. In particular, QDSSCs employing CS 2.5 with thickness of only 64 nm manifest the highest PCE of 3.25%, corresponding to the highest V_{oc} (549 mV), J_{sc} (11.96 mA/cm^2), and *FF* (0.49) as well. To the best of our knowledge, this is the highest PCE achieved using CuS CE with such low thickness in QDSSCs. Moreover, even the QDSSCs assembled with the thinnest CuS CE (CS 1) can obtain a PCE of 2.07%. IPCE measurements of assembled QDSSCs are shown in Fig. 5 (b), all the spectra demonstrate a similar variation trend from 350 to 750 nm, among them, CS 2.5 based QDSSCs yielded higher value in the wavelength of 400–550 nm. Moreover, J_{sc} value of the cells evaluated on the basis of the IPCE spectra is in well consistent with the measured values shown in Table 2.

It can be seen from the above analysis that our thin CuS CEs without any special morphology can show relatively high catalytic performance in S_n^{2-}/S^{2-} redox electrolyte, which is mainly contributed to the high intrinsic catalytic ability of CuS towards the redox couple of S_n^{2-}/S^{2-} [37], resulting from the existence of the van der waals forces between CuS film and polysulfide electrolyte that promote the electrochemical interaction of anions and cations. In other words, CuS CEs with thickness below 100 nm is almost sufficient to catalyze the S_n^{2-}/S^{2-} redox couples in QDSSCs. In addition, there are many advantages of using CEs with low thickness, such as reducing the amount of materials usage, accelerating the charge transfer process in the CE, high binding force with the substrate and the possibility to be applied in bifacial QDSSCs due to high transmittance. For further improving the catalytic performance of CEs, efforts on optimizing CEs can be focused on growing these CuS thin films on the surface of other materials with high conductivity or large surface area like noble metal, carbon materials, and so on, thus to form composite CEs which combine both the high catalytic ability of CuS and superior properties of other materials.

Table. 2
Photovoltaic parameters of QDSSCs using various CEs and electrochemical parameters of EIS measurements based on symmetric cells.

Samples	V_{oc} (mV)	J_{sc} (mA/cm^2)	*FF* (%)	η (%)	R_S (Ω)	R_{ct} (Ω)
CS 1	491 ± 2	9.70 ± 0.10	43.2 ± 0.5	2.07 ± 0.10	13.49 ± 0.16	99.34 ± 0.31
CS 2	524 ± 1	11.51 ± 0.12	43.5 ± 0.4	2.65 ± 0.12	13.15 ± 0.20	77.04 ± 0.25
CS 2.5	549 ± 2	11.96 ± 0.05	49.2 ± ± 0.5	3.25 ± 0.07	12.82 ± 0.12	18.89 ± 0.17
CS 3	538 ± 3	11.64 ± 0.13	47.8 ± 0.6	2.99 ± 0.08	11.40 ± 0.16	58.72 ± 0.27
CS 3.5	532 ± 1	10.48 ± 0.09	48.6 ± 0.2	2.71 ± 0.06	11.11 ± 0.18	60.53 ± 0.26
CS-DB	528 ± 2	11.20 ± 0.08	36.3 ± 0.3	2.15 ± 0.06	33.78 ± 0.25	54.05 ± 0.38
Pt	485 ± 2	9.64 ± 0.14	40.7 ± 0.3	1.91 ± 0.09	10.75 ± 0.13	159.37 ± 0.42

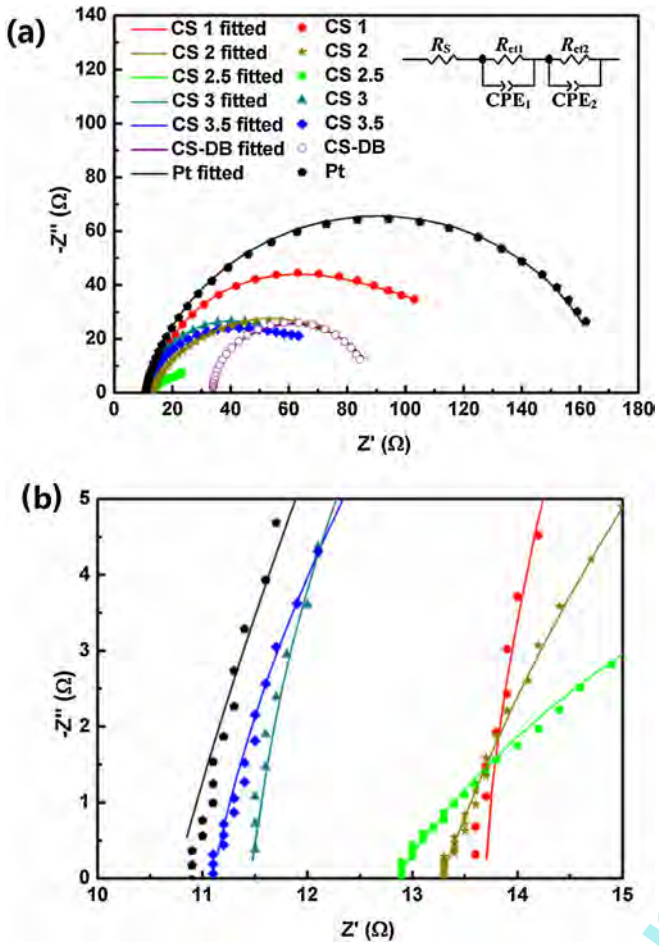

Fig. 6. (a) Nyquist plots of symmetrical dummy cells based on CuS and Pt CEs, the inset is the equivalent circuits of the symmetrical cells. (b) Magnified plots of (a).

3.5. Electrocatalytic and conductive properties

We make further efforts to investigate the dependence of the CuS CEs performance with their thickness. It is well known that CE is where electrons flow back into the electrolyte from external circuit, and it has a vital influence on the solar cell's overall performance [38]. The impact of CE on the performance of QDSSC is mainly derived from the CE material's catalytic ability and its conductivity [39,40]. In the following parts, the catalytic ability and conductivity of CuS CEs with different thickness will be discussed separately.

The catalytic abilities of the CuS CEs with different thickness are firstly evaluated by EIS as well as Tafel testing. EIS measurements are carried on the symmetric cells constructed with two identical electrodes (CE/electrolyte/CE), the obtained spectra were fitted by Z-View software using the equivalent circuit shown in the inset of Fig. 6 (a), and the obtained parameters are exhibited in Table 2. The charge transfer resistances (R_{ct}) reflected from the semicircle in Fig. 6 (a) show that the CuS CEs possess a better electrocatalytic ability that Pt CEs since the R_{ct} of CuS CEs are all smaller than that of Pt CEs. Among the thin CuS CEs, R_{ct} values follow the trend of decreasing from CS 1 (99.34 Ω) to CS 2.5 (18.89 Ω) then increasing to CS 3.5 (60.53 Ω), when the films grow thicker from CS 1 to CS 2.5, the amount of electrode materials for catalyzing the electrolyte increase, so the R_{ct} decrease. From CS 2.5 to CS 3.5, R_{ct} bounce to increase, although the rougher surface of CS 3 and CS 3.5 help to increase the catalytic surface areas, it can be scrutinized from their SEM and AFM images that there are many big particles on the surface, which, from another aspect, reduce the catalytic areas and weaken the catalytic activity of CEs, thus the R_{ct} values increase. Compared with thick CuS CEs, most of the thin CuS CEs possesses higher R_{ct} values than CS-DB (54.05 Ω), indicating that the CS-DB owns a relatively high electrochemical catalytic ability. However, the series resistance of CS-DB is higher than all the thin CuS CE, shown in Fig. 6(b), which may results from the poor contact of the CS-DB with substrate, high R_s value has a negative effects on *FF* [40,41], this results can be also seen in Table 2, the *FF* of CS-DB

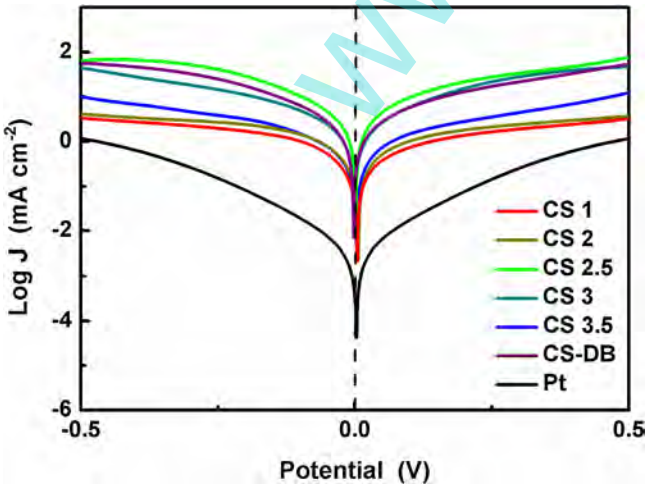

Fig. 7. Tafel plots of different CuS CEs and Pt CEs.

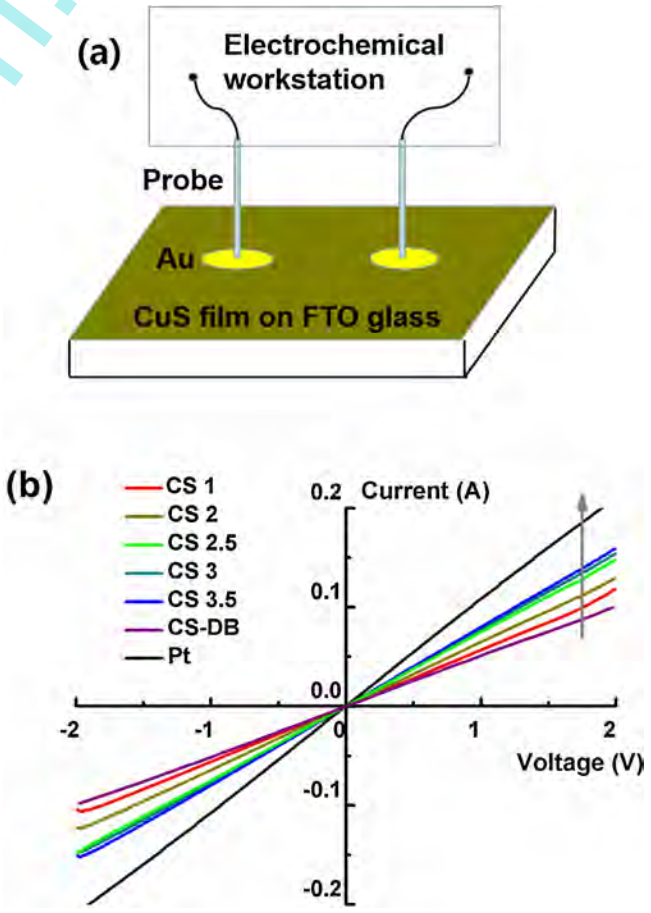

Fig. 8. (a) Schematic image of the device for measuring the resistance of the films. (b) The $I-V$ measured curves of the films.

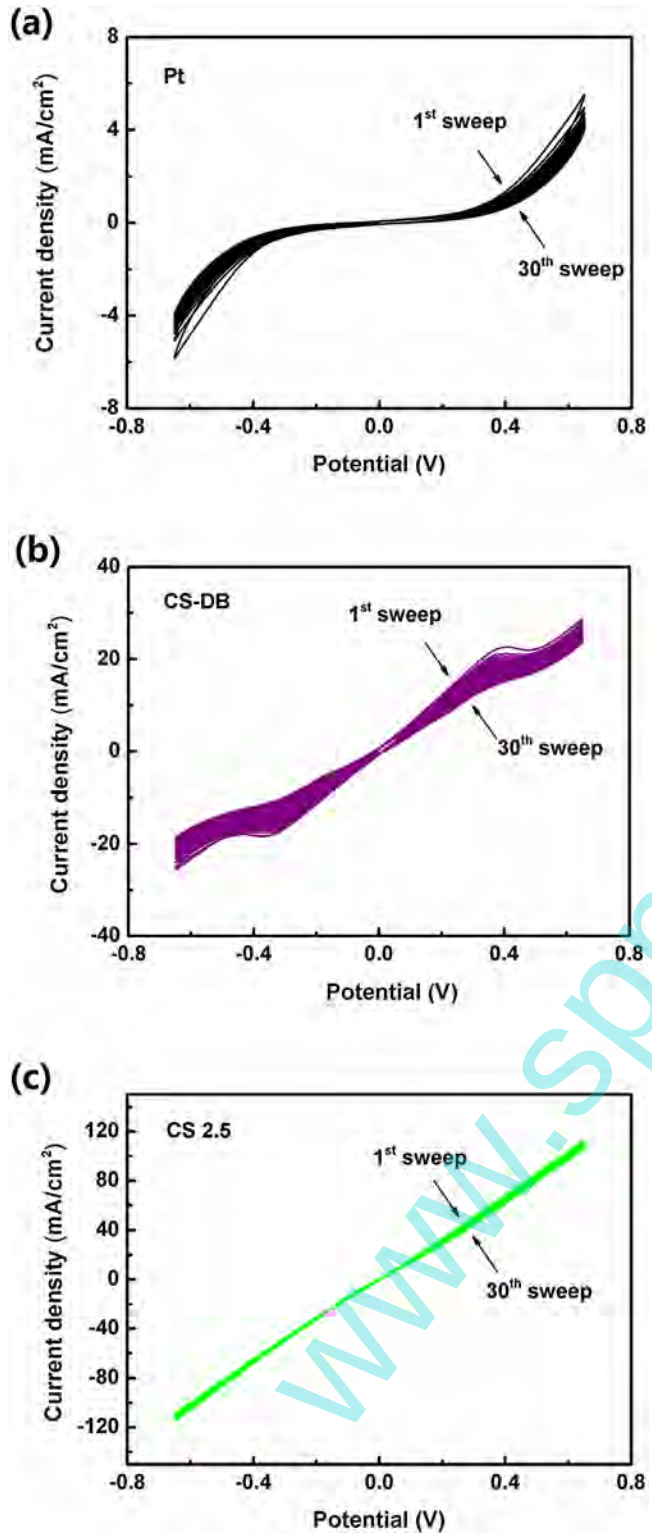

Fig. 9. CV measurements of the symmetrical cells of (a) Pt, (b) CS-DB (c) CS 2.5 for 30 cycles.

assembled QDSSCs is the lowest, thus decreasing the PCE value to a large extent.

Tafel polarization curves also based on the symmetric cells of different CEs are shown in Fig. 7, the intercept by extrapolating the cathodic branches in linear region when the overpotential voltage is zero refers to the exchange current density (J_0), J_0 is a typical parameter to evaluate the electron transfer kinetic and it is also inversely proportional to R_{ct} value on the basis of following formula:

$$J_0 = \frac{RT}{nFR_{ct}} \quad (2)$$

Where R is the gas constant, F is the Faraday constant, T is temperature, n corresponds to the number of electrons involved in preparation, and R_{ct} is the charge transfer resistance. Fig. 7 shows that CuS CEs have larger slope than Pt CEs, implying CuS CEs get a larger J_0 compared to that of Pt CEs, and it also means that CuS CEs have stronger abilities for catalyzing the reduction of polysulfide than Pt CEs. Among CuS CEs, the order of J_0 values is found to be CS 2.5 > CS-DB > CS 3 > CS 3.5 > CS 2 > CS 1, the result is also in agreement with the EIS measurement on the whole. The limiting diffusion current density (J_{lim}) is another parameter to scale the catalytic activity of CEs, it can be obtained from the intersection of cathodic branch and Y-axis, a larger J_{lim} value suggests the CEs own a faster diffusion velocity of S_n^{2-}/S^{2-} at the interface of CE/electrolyte, the order of J_{lim} value is the same as that of J_0, while CS 2.5 CEs holds the highest J_{lim} in consistent with the highest diffusion coefficient towards the redox couple. On the contrary, the lowest J_{lim} of Pt CEs corresponds to the poorest catalytic ability which originated from the catalytic poisoning.

The conductive properties of CEs are investigated as follows, The CE materials with higher conductivity provide more unhindered electron pathways to complete the circuit, and the conductivity of the CE is mainly affected by sheet resistance of the FTO substrate which is the same for all the samples, resistance of the counter electrode material and the corresponding contact resistance [38]. Two-point $I-V$ test in the dark was employed to measure the conductivities of CuS thin films with different thickness, the schematic of the measurement device is depicted in Fig. 8 (a), and the obtained $I-V$ curves are shown in Fig. 8 (b). The characteristics of all the samples are liner, which suggests the formation of Ohmic contacts between the evaporated gold electrodes and the CuS films [42]. It can be deduced that all the resistances of the CuS films are higher than that of Pt films owing to the naturally high conductivity of Pt materials. The resistance of the CS-DB is the highest one, this may be ascribed to its weak adhesion to the substrate. Among the thin CuS films, the resistances keep falling down from CS 1 to CS 3.5, which result from the incensement in thickness of CuS film. Secondly, the contact resistance can be mainly determined by the solar cell's series resistance (R_s). From the EIS measurement results shown in Fig. 6 (b), the R_s value of QDSSCs with different CEs can be obtained from Table 2. The R_s show a corresponding result with Fig. 8 (b), explicitly, from CS 1 to CS 3.5, the R_s values keep decreasing from 13.49 Ω to 11.11 Ω, besides, the R_s of Pt CEs (10.75 Ω) are lower than all the CuS CEs while that of CS-DB is the highest (33.48 Ω). From the above electrochemical analysis, the CS 2.5 has the highest catalytic property and moderate conductivity, which lead to the enhanced solar cell performance.

3.6. Stability

Stability of CEs is another important issue to be considered, 30 cycles of potential sweeping were loaded on different CEs to test their stability in polysulfide electrolyte. It can be observed from Fig. 9 (a) that the CS 2.5 owns a good stability since there is no apparent decay in current density after scanning for 30 cycles. In contrast, the Pt CE and CS-DB decay rapidly after continuous interacting with the electrolyte, inferring their poor stability, this could be attributed to the adsorption of sulfur atoms for Pt and poor contact with substrate for CS-DB. Furthermore, the current density of CS 2.5 is much higher than CS-DB and Pt CEs, which

infers that the CS 2.5 has a higher diffusion velocity, this also corresponds well with the Tafel results.

4. Conclusions

In summary, the CuS thin films prepared via a facile CBD method with thickness around 100 nm have been demonstrated to perform as the efficient CEs in QDSSCs. The highest PCE of 3.25% is achieved by the QDSSCs employing CS 2.5 with thickness of only 64 nm, much higher than the value of QDSSCs using thick CS-DB CEs. Electrochemical analysis also show the 64 nm-thick CE owns a high electrocatalytic activity, good conductivity, and fine stability, which infers that CuS CEs with thickness below 100 nm are sufficient to catalyze the S_n^{2-}/S^{2-} redox couples. Based on the superiority of thin films, improvements could be focused on growing thin CuS films on other materials like reduced graphene oxide, CoS and so on to further enhance the electrocatalytic performance of CEs and the PCE of QDSSCs.

Acknowledgements

Financial support from the National Natural Science Foundation of China (Grant No. 61306082 and 61306083), the China Postdoctoral Science Foundation (Grant No. 2014M561845), Key Laboratory of Functional Crystals and Laser Technology, TIPC, CAS, and Anhui Provincial International Science and Technology Cooperation Program (10080703021) is acknowledged.

References

[1] I. Hwang, K. Yong, ChemElectroChem 2 (2015) 634.
[2] I. Hdd, A. Zaban, Langmuir 30 (2013) 7264.
[3] Z. Yang, C.-Y. Chen, C.-W. Liu, H.-T. Chang, Chem. Commun. 46 (2010) 5485.
[4] G. Hodes, J. Manassen, D. Cahen, J. Electrochem. Soc. 127 (1980) 544.
[5] M. Seol, E. Ramasamy, J. Lee, K. Yong, J. Phys. Chem. C 115 (2011) 22018.
[6] M.-H. Yeh, C.-P. Lee, C.-Y. Chou, L.-Y. Lin, H.-Y. Wei, C.-W. Chu, R. Vittal, K.-C. Ho, Electrochimica. Acta 57 (2011) 277.
[7] M. Wu, X. Lin, T. Wang, J. Qiu, T. Ma, Energy Environ. Sci. 4 (2011) 2308.
[8] M.-H. Yeh, C.-P. Lee, C.-Y. Chou, L.-Y. Lin, H.-Y. Wei, C.-W. Chu, R. Vittal, K.-C. Ho, Electrochimica. Acta 57 (2011) 277284.
[9] X. Huang, S. Huang, Q. Zhang, X. Guo, D. Li, Y. Luo, Q. Shen, T. Toyoda, Q. Meng, Chem. Commun. 47 (2011) 2664.
[10] W. Chen, M. Wang, T. Qian, H. Cao, S. Huang, Q. He, N. Liang, C. Wang, J. Zai, Nano Energy 12 (2015) 186.
[11] A.D. Savariraj, K.K. Viswanathan, K. Prabakar, ACS Appl. Mater. Interfaces 6 (2014) 19702.
[12] M. Ye, X. Wen, N. Zhang, W. Guo, X. Liu, C. Lin, J. Mater. Chem. A 3 (2015) 9595.
[13] H. Zhang, H. Bao, X.-H. Zhong, J. Mater. Chem. A 3 (2015) 6557.
[14] A.D. Mani, M. Deepa, P. Ghosal, C. Subrahmanyam, Electrochimica. Acta 139 (2014) 365.
[15] H. Yuan, J. Lu, X. Xu, D. Huang, W. Chen, Y. Shen, M. Wang, J. Electrochem. Soc. 160 (2013) 624.
[16] Y. Zhang, C. Shi, X. Dai, F. Liu, X. Fang, J. Zhu, Electrochimica. Acta 118 (2014) 41.
[17] X.-W. Zeng, D.-H. Xiong, W.-J. Zhang, L.-Q. Ming, Z. Xu, Z.-F. Huang, M.-K. Wang, W. Chen, Y.-B. Cheng, Nanoscale 5 (2013) 6992.
[19] G. Hodes, J. Manassen, D. Cahen, Nature 261 (1976) 403.
[20] S. Gimenez, I. Mora-Sero, L. Macor, N. Guijarro, T. Lana-Villarreal, R. Gomez, L.J. Diguna, Q. Shen, T. Toyoda, J. Bisquert, Nanotechnology 20 (2009) 295204.
[21] P. Lukashev, W.R. Lambrecht, T. Kotani, M.V. Schilfgaarde, Phys. Rev. B 76 (2007) 195202.
[22] C.S. Kim, S.H. Choi, J.H. Bang, ACS Appl. Mater. Interfaces 6 (2014) 22078.
[23] J. Xu, J. Xiao, J. Dong, Y. Luo, D. Li, Q. Meng, Electrochim. Acta 127 (2014) 180.
[24] W. Ke, G. Fang, H. Lei, P. Qin, H. Tao, W. Zeng, J. Wang, X. Zhao, J. Power. Sources 248 (2014) 809.
[25] A. Hauch, A. Georg, Electrochimica Acta 46 (2001) 3457.
[26] S. Ito, T.N. Murakami, P. Comte, P. Liska, C. Grätzel, M.K. Nazeeruddin, M. Grätzel, Thin Solid Films 516 (2008) 4613.
[27] S. Wang, W. Dong, X. Fang, S. Wu, R. Tao, Z. Deng, J. Shao, L. Hu, J. Zhu, J. Power. Sources 273 (2015) 645.
[28] S.-M. Wang, W.-W. Dong, R.-H. Tao, Z.-H. Deng, J.-Z. Shao, L.-H. Hu, J. Zhu, X.-D. Fang, J. Power. Sources 235 (2013) 193.
[29] S. Wang, W. Dong, X. Fang, S. Zhou, J. Shao, Z. Deng, R. Tao, Q. Zhang, L. Hu, J. Zhu, Electrochimica Acta 154 (2015) 47.
[30] P.K. Nair, M.T.S. Nair, V.M. Garcıa, O.L. Arenas, Y. Pena, A. Castillo, I.T. Ayala, O. Gomezdaza, A. Sanchez, J. Campos, H. Hu, R. Suarez, M.E. Rincon, Sol. Energy Mater. Sol. Cells 52 (1998) 313.
[31] J. Dona, J. Herrero, Journal Electrochem Soc. 144 (1997) 4081.
[32] R.S. Mane, C.D. Lokhande, Mater. Chem. Phys. 65 (2000) 1.
[33] R. Ortega-borges, D. Lincot, J. Electrochem. Soc. 140 (1993) 3464.
[34] S.K. Maji, N. Mukherjee, A.K. Dutta, D.N. Srivastava, P. Paul, B. Karmakar, A. Mondal, B. Adhikary, Mater. Chem. Phys. 130 (2011) 392.
[35] F.I. Ezema, D.D. Hile, S.C. Ezugwu, R.U. Osuji, P.U. Asogwa, J. Ovonic. Res. 6 (2010) 99.
[36] S.H. Chaki, M.P. Deshpande, J.P. Tailor, Thin. Solid. Films 550 (2014) 291.
[37] P.V. Kamat, J. Phys. Chem. Lett. 4 (2013) 908.
[38] S.-Q. Fan, B. Fang, J.H. Kim, J.-J. Kim, J.-S. Yu, J. Ko, Appl. Phys. Lett. 96 (2010) 063501.
[39] L.T.L. Lee, J. He, B. Wang, Y. Ma, K.-Y. Wong, Q. Li, X. Xiao, T. Chen, Sci. Rep. 4 (2014) 4063.
[40] G. r. Li, F. Wang, Q.W. Jiang, X. p. Gao, P. w. Shen, Angew. Chem. Int. Ed. 49 (2010) 3653.
[41] K. Meng, G. Chen, R. Thampi, J. Mater. Chem. A 3 (2015) 23074.
[42] J.M. Bian, X.M. Li, C.Y. Zhang, L.D. Chen, Q. Yao, Appl. Phys. Lett. 84 (2004) 3783.